

See discussions, stats, and author profiles for this publication at: <https://www.researchgate.net/publication/244278825>

Theoretical study on selective oxidation of olefin and alcohol with Mo–peroxo amine complex using “paired interacting orbitals (PIOs)” analysis

ARTICLE *in* JOURNAL OF MOLECULAR CATALYSIS A CHEMICAL · AUGUST 2008

Impact Factor: 3.62 · DOI: 10.1016/j.molcata.2008.05.012

CITATIONS

3

READS

19

2 AUTHORS, INCLUDING:



Akinobu Shiga

LUMMOX Research Lab.

48 PUBLICATIONS 676 CITATIONS

SEE PROFILE



Theoretical study on reaction between bis(μ -peroxo)dicopper(2)complex and phenol by “paired interacting orbitals (PIO)” analysis

Akinobu Shiga^{a,*}, Yasuhiko Kurusu^b

^a LUMMOX Laboratory, Takezono 2-18-4-302, Tsukuba 3050032, Japan

^b Sophia University, Faculty of Science and Technology (Emeritus Professor),
187-104 Honnumoku Mannsaka, Naka-ku, Yokohama 231-0833, Japan

Received 12 January 2005; received in revised form 26 June 2005; accepted 29 June 2005

Abstract

The reaction between μ - η^2 : η^2 -dibridging peroxodicopper complex of bis[3-(2-hydroxybenzylideneamino)phenyl]sulfone and phenol are investigated by performing paired interacting orbitals (PIO) analysis proposed by Fujimoto et al. Perusal of the contour maps and overlap populations of main PIOs suggested that formation of mono-phenoxo complex is easy; however di-phenoxo complex formation is difficult because of the non-flexibility of the SO_2 -bridged ligand. This result supplies the reason why poly (phenylene oxide) was not formed in our system.

© 2005 Elsevier B.V. All rights reserved.

Keywords: (μ -Peroxo)dicopper complex; Phenoxodicopper complex; Phenol; Reaction mechanism; Paired interacting orbitals (PIO) analysis

1. Introduction

Dinuclear copper complexes were active for phenol oxidation, whose active species were produced by their reaction with hydrogen peroxide, *t*-butyl hydroperoxide or other oxidants. The proposed active intermediate is shown in Scheme 1 [1]. Synthesis of peroxodicopper complex was reported by Kitajima et al. [2]. Related similar reports are reviewed recently [3].

Here we synthesized a new type of copper complexes from salicylaldehyde and bis(3-aminophenyl)sulphone followed by complex formation with copper acetate. The bis(μ -peroxo)dicopper active species was supposed from the reaction route [I] shown in Scheme 2. It is shown how the active species oxidize phenol in this report. We suggest the oxidation route [II] of Scheme 2. We tried to clearly show an activation route of the reaction between μ - η^2 : η^2 -dibridging peroxide

and phenols by paired interacting orbitals (PIO) analysis by Fujimoto et al. [4]. Thus we simulate the reaction of hydrogen peroxide with the copper dinuclear complex and also estimated the reaction coordinate for the interaction between phenols and the active intermediate site.

2. Models and calculation methods

2.1. Modeling of copper dinuclear complex

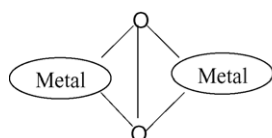
A molecular structure of the copper dinuclear complex was estimated by using the Z-matrix method. Adjusting the bridge angle of $\angle\text{CSC}$ and comparing the calculated structure with the reported results [3], we determined the model structure.

A schematic illustration of the copper dinuclear complex is shown in Fig. 1.

Determined structural parameters are as followings: $\text{Cu}-\text{Cu} = 3.12 \text{ \AA}$, $\text{Cu}-\text{O}^* = 1.90 \text{ \AA}$, $\text{O}^*-\text{O}^{**} = 2.18 \text{ \AA}$,

* Corresponding author. Tel.: +81 90 17335602.

E-mail addresses: aas55@mail2.accsnet.ne.jp (A. Shiga),
GZS00125@nifty.ne.jp (Y. Kurusu).



Scheme 1. Dibridging peroxide.

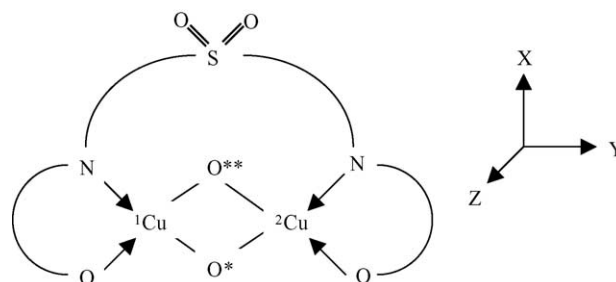


Fig. 1. A schematic illustration of the dicopper(2) complex.

51 $\text{Cu}-\text{O}=2.55 \text{ \AA}$, $\text{Cu}-\text{N}=2.32 \text{ \AA}$, $\angle \text{CuO}^{**}\text{Cu}=110^\circ$,
 52 $\angle \text{O}^*\text{CuO}^{**}=70^\circ$, $\angle \text{CSC}=90.0^\circ$.

53 2.2. Investigation of reaction path between the copper 54 dinuclear complex and phenol

55 We determined the position of phenol in X–Y, X–Z, and
 56 Y–Z plains in front and back of the O^* atom. It was found
 57 that the position in which hydrogen of hydroxyl group of
 58 phenol was put in the X–Z plane in front of O^* is suitable
 59 for phenol coordination to the copper dinuclear complex. We
 60 elongated the H–O distance of phenol and moved the O–Ph
 61 moiety to the ^2Cu atom. We employed eight states along the
 62 assumed reaction path. The distance of H–O of phenol:R1,
 63 the distance of O^*-H :R2, the distance between O of phenol
 64 and O^* :R3, and the distance between O of phenol and ^2Cu
 65 atom:R4 of each state are shown in Table 1.

66 Two examples of the states are shown in Fig. 2.

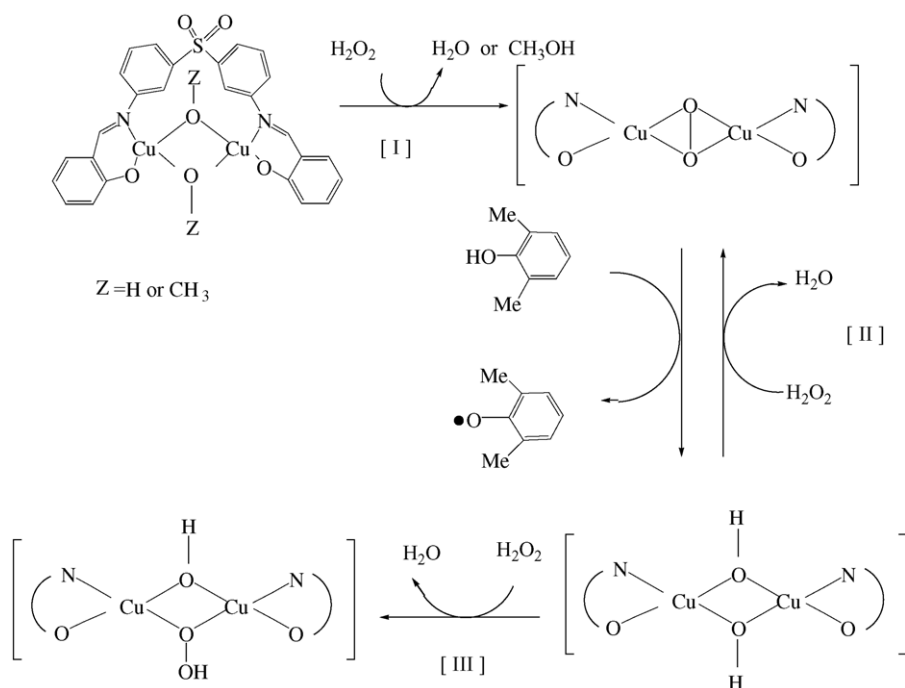
67 2.3. PIO calculation

68 For PIO analysis extended Hückel MO calculation was
 69 carried out. The extended Hückel parameters are given

in Appendix A. All calculations were carried out on
 LUMMOXTM system [5]. Nowadays, it is not so difficult to
 carry out ab initio MO calculation as before; however, there
 are still some inconveniences. The accuracy and the calculation
 time are largely dependent on the basis sets used; the
 larger are the basis sets, the more accurate the calculation
 result, but the more time consuming, moreover, the more difficult
 to understand the composition of MOs. Although PIO
 analysis was proposed originally for ab initio calculations,
 we already reported that this approach was also useful in ana-

Table 1
The distances: R1, R2, R3 and R4, of each state

State NO (Å)	(00)	(01)	(02)	(03)	(04)	(05)	(06)	(07)
R1	0.96	1.28	1.44	1.63	1.52	1.72	1.72	1.81
R2	1.98	1.89	1.89	1.89	1.89	1.89	1.49	1.10
R3	2.93	2.93	3.01	3.11	2.67	2.49	2.21	2.14
R4	3.66	3.66	3.59	3.54	3.04	2.62	2.22	2.00



Scheme 2. Formation of active intermediate.

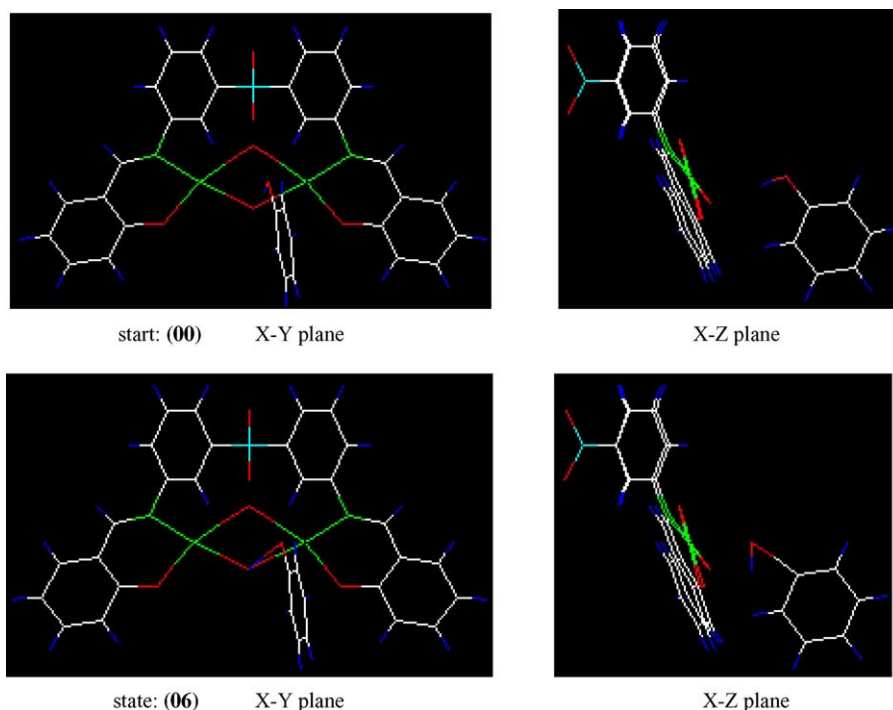


Fig. 2. Examples of the states along with the reaction path.

lyzing the results of extended Hückel MO calculations and was suitable for understanding reaction procedures in terms of orbital interactions, especially in catalytic systems large in size. [6] We also reported that relative catalytic activities deduced from PIO analysis based on extended Hückel MO calculations coincided with the order of activation energy obtained from ab initio MO calculations [7]. We divide a model complex (combined system C) into a catalyst portion (fragment A) and an attacking molecule portion (fragment B). Here, the fragment A is the Cu complex and the fragment B is phenol. The geometries of [A] and [B] are the same as those in the original complex ([A + B] \equiv [C]).

The MOs of [A], [B] and [C] are calculated and PIOs are obtained by applying the procedure that was proposed by Fujimoto et al. [4]. It is summarized as follows:

- (1) We expand the MOs of a complex in terms of the MOs of two fragment species, to determine the expansion coefficients c_{if} , c_{m+jf} and d_{kf} , d_{n+lf} in Eq. (1)

$$\begin{aligned} \Phi_f = & \sum_{i=1}^m c_{i,f} \phi_i + \sum_{j=1}^{M-m} c_{m+j,f} \phi_{m+j} \\ & + \sum_{k=1}^n d_{k,f} \psi_k + \sum_{l=1}^{N-n} d_{n+l,f} \psi_{n+l}, \\ f = & 1, 2, \dots, m+n \end{aligned} \quad (1)$$

$$\begin{array}{c} \begin{array}{|c|} \hline \begin{array}{c} \Phi(\text{occ}) \\ \Phi: \text{MO of C} \\ C \equiv A + B \end{array} \\ \hline \end{array} = \begin{array}{|c|} \hline \begin{array}{c} \phi(\text{unocc}) \\ \phi; \text{MO of A} \end{array} \\ \hline \end{array} + \begin{array}{|c|} \hline \begin{array}{c} \psi(\text{unocc}) \\ \psi: \text{MO of B} \end{array} \\ \hline \end{array} \\ + \begin{array}{|c|} \hline \begin{array}{c} \phi(\text{occ}) \\ \phi; \text{MO of A} \end{array} \\ \hline \end{array} + \begin{array}{|c|} \hline \begin{array}{c} \psi(\text{occ}) \\ \psi: \text{MO of B} \end{array} \\ \hline \end{array} \end{array}$$

- (2) We construct an interaction matrix P which represents the interaction between the MOs of the fragment [A] and the MOs of the fragment [B]

$$P = \begin{pmatrix} p_{i,k} & p_{i,n+l} \\ p_{m+j,k} & p_{m+j,n+l} \end{pmatrix} \quad (2)$$

in which

$$p_{i,k} = n_{t,u} \sum_{f=1}^{m+n} c_{i,f} d_{k,f}, \quad i = 1 \sim m, k = 1 \sim n$$

$$p_{i,n+l} = n_{t,u} \sum_{f=1}^{m+n} c_{i,f} d_{n+l,f},$$

$$i = 1 \sim m, l = 1 \sim N - n$$

$$p_{m+j,k} = n_{t,u} \sum_{f=1}^{m+n} c_{m+j,f} d_{k,f},$$

$$j = 1 \sim M - m, k = 1 \sim n$$

$$p_{m+j,n+l} = n_{t,u} \sum_{f=1}^{m+n} c_{m+j,f} d_{n+l,f},$$

$$j = 1 \sim M - m, l = 1 \sim N - n$$

- (3) We obtain transformation matrix U^A (for A) and U^B (for B) by

$$\tilde{P} P U^A = U^A \Gamma \quad (3)$$

$$U^B = (\gamma_v)^{-\frac{1}{2}} \sum_r p_{r,v} U_{r,v}^A, \quad v = 1, 2, \dots, N \quad (4)$$

- (4) And finally we obtain the PIOs by Eqs. (5) and (6)

$$\phi'_v = \sum_r^N U_{r,v}^A \phi_r \quad (\text{for A}) \quad (5)$$

$$\psi'_v = \sum_s^N U_{s,v}^B \psi_s \quad (\text{for B}) \quad (6)$$

The $N \times M$ ($N < M$) orbital interactions in the complex C can thus be reduced to the interactions of N PIOs, N indicating the smaller of the numbers of MOs of the two fragments, A and B.

3. Results

3.1. Phenol addition

The eigen values and overlap population of PIOs of phenol addition on ($\text{Cu}_2\text{O}_2\text{L}$) are shown in Tables 2 and 3, respectively.

An eigen value of PIO means the contribution of the PIO to the interaction. Table 2 tells us that the interaction between ($\text{Cu}_2\text{O}_2\text{L}$) and phenol is expressed by one major interaction (PIO-1) in the states (0 1), (0 2) and (0 3), by two major interactions (PIO-1 and PIO-2) in the states (0 4) and (0 5) and by three major interactions (PIO-1, PIO-2 and PIO-3) in the states (0 6) and (0 7). The overlap population of each PIO and the sum of all PIOs (ΣOP) are shown in Table 3. The ΣOP of each state is almost the same as the sum of overlap population of those major contributing PIOs. We use the ΣOP as an indicator of the reaction. The larger the ΣOP value, the more favorably the addition takes place.

Table 2
The eigen values of PIOs of the each state

State NO	(00)	(01)	(02)	(03)	(04)	(05)	(06)	(07)
PIO-1	–	0.0679	0.1136	0.2443	0.1300	0.2027	0.3907	0.3770
PIO-2	–	0.0053	0.0065	0.0070	0.0089	0.0237	0.0848	0.1893
PIO-3	–	0.0004	0.0003	0.0004	0.0026	0.0146	0.0337	0.1528
PIO-4	–	0.0001	0.0001	0.0002	0.0018	0.0097	0.0039	0.0328
PIO-5	–	–	–	–	0.0003	0.0016	0.0023	0.0150
PIO-6	–	–	–	–	0.0001	0.0007	0.0014	0.0129

Table 3
The overlap population and total overlap population (ΣOP) of all PIOs of the each state

State NO	(00)	(01)	(02)	(03)	(04)	(05)	(06)	(07)
PIO-1	–	0.0411	0.0562	0.0827	0.0560	0.0653	0.2226	0.4725
PIO-2	–	–0.0068	–0.0082	–0.0080	–0.0107	–0.0002	0.0394	–0.1274
PIO-3	–	–0.001	–0.0001	–0.0002	0.0018	–0.0055	–0.0267	0.1197
PIO-4	–	–	0.0001	0.0001	–0.0012	–0.0075	–0.0032	–0.0376
PIO-5	–	–	–	–	–0.0003	–0.0017	–0.0014	–0.0125
PIO-6	–	–	–	–	–	–0.0003	–0.0004	–0.0060
⋮	–	–	–	–	–	–	–	–
PIO-30	–	–	–	–	–	–	–	–
ΣPIO	–	0.0342	0.0480	0.0746	0.0456	0.0500	0.2297	0.4077

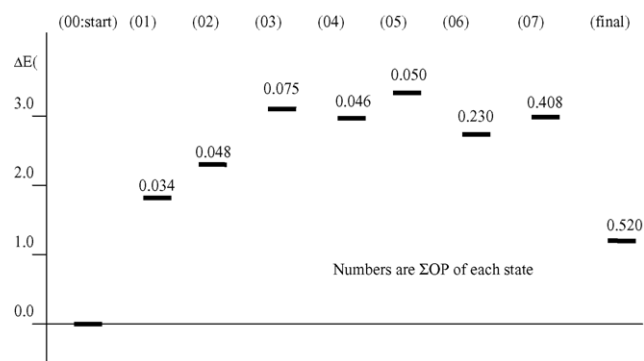


Fig. 3. An energy diagram of phenol addition on ($\text{Cu}_2\text{O}_2\text{L}$).

The energy diagram of phenol addition to ($\text{Cu}_2\text{O}_2\text{L}$) is shown in Fig. 3. According to the elongation of the H–O distance of phenol, the combined total system becomes unstable; however because of the shortening of the distance between the oxygen of phenol and the ^2Cu atom, the ΣOP increases gradually. The ΣOP of the states (06) and (07) increase markedly. This suggests the formation of mono-phenoxodicopper(2) complex. The contour maps of the most important top three PIOs: PIO-1, PIO-2, and PIO-3 of (07) are shown in Fig. 4. The PIO-1 represents the bonding interaction between the hydrogen of phenol and O^* of the complex. We can see also the anti-bonding interaction between the phenol hydrogen and phenol oxygen. This means that the bond breaking of phenol hydrogen is taking place. The PIO-

2 represents the anti-bonding interaction between the phenyl group of phenol and the O atom of the ligand. The PIO-3 represents the bonding interaction between the oxygen of phenol and the ^2Cu atom. And finally reaching the formation of mono-hydroxo-, mono-phenoxodicopper(2) complex, the whole system is strongly stabilized. From this, we can estimate the formation of phenoxo– ^2Cu bond in the final state.

3.2. Second phenol addition

Here we examine second phenol addition to mono-phenoxodicopper(2) complex. First we started from the mono-hydroxo-, mono-phenoxodicopper(2) complex. However the phenol coordination was very difficult because of the steric hindrance caused by the hydroxyl group. So we start from the state (07) of mono-phenoxodicopper(2) complex. We put a hydrogen of hydroxyl group of phenol in front of O^* atom on the Z-axis in X–Z plane and take the same deformation process as mentioned in Section 2.2. We employ four states: (00'), (01'), (04'), and (07').

Total energies (E_c) and ΣOP of each state of second phenol addition are summarized in Table 3. The instability (ΔE) from (00') to (07') is of the same order of magnitude as that from (00) to (07); however the increase in ΣOP from (00') to (07') of (0.0874) is markedly smaller than that from (00) to (07) of (0.4077). This implies that the same order of the activation is still far insufficient for second phenoxo complex

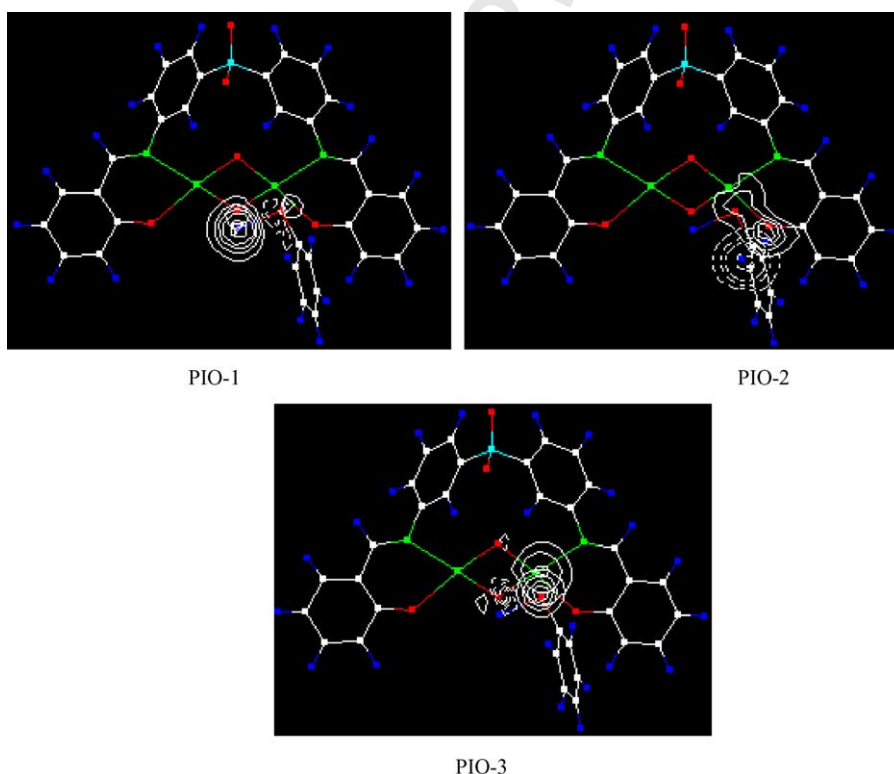


Fig. 4. The contour maps of top three PIOs: PIO-1, PIO-2, and PIO-3 of (07).

Table 4

Total energies (E_c) and total overlap population (ΣOP) of phenol adsorption on $(Cu_2O_2L)(C_6H_5OH)$; $\Delta E = E_c$ (each state) $- E_c$ (0 0:start)

Sample states	E_c (eV)	ΔE (eV)	ΣOP
(0 0':start)	−4929.00	0.0	–
(0 1')	−4928.35	+0.65	0.0064
(0 4')	−4925.85	+3.15	0.0172
(0 7')	−4925.99	+3.01	0.0874

formation. From this, we can estimate that the second phenol addition does not take place.

4. Discussion

4.1. Why does not PPE formation takes place?

Several years ago Higashimura et al. reported that 2- and/or 6 unsubstituted phenols were oxidatively polymerized to structurally regulated poly(1,4-phenylene oxide)s by using a (1,4,7-triisopropyl-1,4,7-triazacyclononane)copper(2)complex catalyst [8]. They called it “radical-controlled” oxidative polymerization. Recently according to ab initio calculation, Kubota et al. have proposed that the key intermediate of the radical-controlled polymerization is phenoxocopper(2)complex [9]. It is supposed that the relative tandem position of two phenoxo groups is crucial for the formation of poly(1,4-phenylene oxide)s and such a position is rather easily attained in the case of the phenoxodicopper(2)complex which is obtained from the reaction between μ - η^2 , η^2 -peroxo-(1,4,7-triisopropyl-1,4,7-triazacyclononane)copper(2)complex and phenol because of the flexibility of the triazacyclononane ligand. On the other hand, it is difficult to form a kind of diphenoxo complex in the case of the copper dinuclear complex: $(CuO)_2SO_2(C_6H_4NCHC_6H_4O)_2$ because of the non-flexibility of the SO_2 -bridged ligand. As a result, it is difficult to attain the tandem position of two phenoxo groups, and the regulated head to tail polymerization of phenols is impossible (Table 4).

5. Conclusion

The reaction between μ - η^2 : η^2 -dibridging peroxydicopper complex of bis[3-(2-hydroxybenzylideneamino)-phenyl]sulfone and phenol are investigated by using PIO analysis proposed by Fujimoto et al.[4].

- (1) Perusal of the contour maps and overlap populations of main PIOs suggested that formation of mono-phenoxo complex is easy whereas di-phenoxo complex formation is difficult.
- (2) The reason why the di-phenoxo complex formation is difficult is the non-flexibility of the SO_2 -bridged ligand.

- (3) The reason why the formation of poly(phenylene oxide) is impossible in this catalyst system may be the difficulty of di-phenoxo complex formation.
- (4) PIO analysis of extended Hückel MO calculations is a fast and informative method for understanding reaction mechanism in terms of orbital interactions, especially in catalytic systems large in size.

Appendix A

Coulomb Integrals and orbital exponents are listed in Table 5.

Table 5

Extended Hückel parameters

Orbital	H_{ii} (eV)	ζ_1	ζ_2
H1s	−13.60	1.300	
C2s	−21.40	1.625	
C2p	−11.40	1.625	
N2s	−26.00	1.950	
N2p	−13.40	1.950	
O2s	−32.30	2.275	
O2p	−14.80	2.275	
S3s	−20.00	1.817	
S3p	−13.30	1.817	
Cu4s	−11.40	2.200	
Cu4p	−6.06	2.200	
Cu3d	−14.00	5.950	0.5933
		2.300	0.5744

References

- [1] (a) A.M. Guidote Jr., K. Ando, Y. Kurusu, H. Nagao, Y. Masuyama, Inorg. Chim. Acta 314 (2001) 27–36;
(b) A.M. Guidote Jr., K. Ando, K. Terada, Y. Kurusu, H. Nagao, Y. Masuyama, Inorg. Chim. Acta 324 (2001) 203–211.
- [2] N. Kitajima, Y. Moro-oka, Chem. Rev. 94 (1994) 737.
- [3] (a) L.M. Mirika, X. Ottenwaelder, T.D.P. Stack, Chem. Rev. 104 (2004) 1013;
(b) E.A. Lewis, W.B. Tolman, Chem. Rev. 104 (2004) 1047.
- [4] (a) H. Fujimoto, T. Yamasaki, H. Mizutani, N. Koga, J. Am. Chem. Soc. 107 (1985) 6157;
(b) H. Fujimoto, Acc. Chem. Res. 20 (1987) 448.
- [5] H. Katsumi, Y. Kikuzono, M. Yoshida, A. Shiga, H. Fujimoto, Sumitomo Chemical Co. Ltd., Tokyo 1999.
- [6] (a) A. Shiga, J. Kojima, T. Sasaki, Y. Kikuzono, J. Organomet. Chem. 345 (1988) 275;
(b) A. Shiga, H. Kawamura, T. Ebara, T. Sasaki, Y. Kikuzono, J. Organomet. Chem. 366 (1989) 95;
(c) A. Shiga, J. Mol. Catal. A 146 (1999) 325;
(d) T. Motoki, A. Shiga, J. Comput. Chem. 25 (2004) 106.
- [7] A. Shiga, J. Macromol. Sci. A34 (1997) 1867.
- [8] H. Higashimura, K. Fujisawa, Y. Moro-oka, M. Kubota, A. Shiga, A. Terahara, H. Uyama, S. Kobayashi, J. Am. Chem. Soc. 120 (1998) 8529.
- [9] M. Kubota, A. Shiga, H. Higashimura, K. Fujisawa, Y. Moro-oka, H. Uyama, S. Kobayashi, Bull. Chem. Soc. Jpn. 77 (2004) 813.